Earthq Eng & Eng Vib (2010) 9: 177-187 **DOI**: 10.1007/s11803-010-0004-6

Earthquake-induced landslide displacement attenuation models and application in probabilistic seismic landslide displacement analysis

Zhang Jian[1†], Cui Peng[2‡], Zhang Bingkun[1§], Yang Changwei[1§] and Graeme H. McVerry[3‡]

1. *Southwest Jiaotong University, Chengdu 610031, China*
2. *Institute of Mountainous and Disaster, Chinese Academy of Sciences, Chengdu 610041, China*
3. *GNS Science, PO BOX 30368, Lower Hutt, New Zealand*

Abstract: A landslide displacement (D_{LL}) attenuation model has been developed using spectral intensity and a ratio of critical acceleration coefficient to ground acceleration coefficient. In the development of the model, a New Zealand earthquake record data set with magnitudes ranging from 5.0 to 7.2 within a source distance of 175 km is used. The model can be used to carry out deterministic landslide displacement analysis, and readily extended to carry out probabilistic seismic landslide displacement analysis. D_{LL} attenuation models have also been developed by using earthquake source terms, such as magnitude and source distance, that account for the effects of earthquake fault type, source type, and site conditions. Sensitivity analyses show that the predicted D_{LL} values from the new models are close to those from the Romeo model that was developed from an Italian earthquake record data set. The proposed models are also applied to an analysis of landslide displacements in the Wenchuan earthquake, and a comparison between the predicted and the observed results shows that the proposed models are reliable, and can be confidently used in mapping landslide potential.

Keywords: displacement; landslide; intensity measures; deterministic analysis; probabilistic analysis

1 Introduction

Earthquake-induced landslides are one of the most important seismic hazards that often result in serious structural damage and loss of life. To identify potential losses from earthquake-induced landslides, an approach often used is to map a parameter that can represent landslide potential. Landslide displacement (D_{LL}) is one of the parameters that can be derived from the Newmark displacement model (1965). Therefore, D_{LL} is sometimes called the Newmark displacement. Two types of D_{LL} models, expressed by either seismic intensity or earthquake source parameters, are often used to estimate landslide displacements. The first type of models includes the Jibson *et al*. model (1998) (using the Arias intensity, I_a) and the Crespellani *et al*. model (1998) (using an earthquake destructiveness potential factor, P_a). The second type of model includes the Ambraseys & Srbulov model (Ambraseys and Srbulov, 1994) and the Romeo model (Romeo, 2000). On the basis of existing D_{LL} models, some landslide-potential maps have been developed and used in landslide hazard mitigation strategies. However, some drawbacks still exist in the existing D_{LL} models. For example, the effects of faulting mechanism and tectonic type are not included in the existing D_{LL} models. However, it is well-known that faulting mechanism and tectonic type have a strong effect on ground motions. In addition, few existing models include the effect of vibration frequency on landslide displacement, but experiments (Wartman *et al*., 2001) showed that this effect is significant. The existing landslide displacement attenuation models can not be easily used in a simplified probabilistic seismic landslide displacement analysis (PSLDA), such as in the model by Romeo (2000), because the ground response intensity used in the existing models, such as Arias Intensity, can not be easily estimated from a widely used probabilistic seismic hazard analysis (PSHA). Therefore, some modifications to the existing D_{LL} models are necessary.

In the present study, two types of D_{LL} models are developed, one using spectral intensity and the other using earthquake source parameters to account for the effects of tectonic type and faulting mechanism. A New

Correspondence to: Zhang Jian, Southwest Jiaotong University, Chengdu 610031, China
Tel: +86-28-87603978;
E-mail: JianZhang1102@home.swjtu.edu.cn
†Professor; ‡Principal Scientist; §Post-graduate Student

Supported by: Foundation for Research and Science and Technology of New Zealand, No C05X0208 and C05X0301; Major Project of Chinese National Programs for Fundamental Research and Development (973 Program), No 2008CB425802

Received February, 2, 2010; **Accepted** April 19, 2010

Zealand earthquake record data set is used to develop the D_{LL} models in the study. The reason for using the spectral intensity in this study, rather than the Arias Intensity, is that the spectral intensity incorporates the effect of vibration frequencies and vibration amplitude, and more importantly the spectral intensity is easily obtained from PSHA. Note that the first type of D_{LL} model developed in the study is easily extended to perform simplified PSLDA, and the second type of D_{LL} model can be directly used to develop truly probabilistic seismic landslide displacement models. Finally, the predicted landslide displacements from the model are compared with observed landslide displacements, including those from the Wenchuan earthquake.

2 Newmark displacement model and ground response intensity

2.1 Newmark displacement model

The Newmark displacement model is often used to estimate the total permanent displacement for slope failures triggered by earthquakes, where permanent displacement occurs only when the earthquake acceleration acting on the assumed rigid friction block exceeds its critical acceleration. Therefore, the critical acceleration is an important factor, depending on topography of the slope and soil properties, and can be estimated as follows:

$$k_c=(\mathrm{FS}-1)\sin\alpha \tag{1}$$

where k_c is the critical acceleration in g (gravity acceleration), FS is the static factor of safety, and α is the angle between the slip direction of the mass centre and the horizontal direction.

As known from slope stability analysis, the static factor of safety is dependent on the geometric shape of a failure surface in the slope, and a failure surface is often assumed as either an infinite, planar, circular or compound surface. An infinite failure surface assumption is often used in landslide hazard mapping for the sake of simplicity, but using this assumption implies: 1) the thickness of the landslide block is much smaller than its length; and 2) the failure surface is parallel to the ground surface. On the basis of an infinite failure surface assumption, the static factor of safety can be estimated from Eq. (2):

$$\mathrm{FS}=\frac{c'}{\gamma t\sin\alpha}+\frac{\tan\phi'}{\tan\alpha}-\frac{m\gamma_w\tan\phi'}{\gamma\tan\alpha} \tag{2}$$

where φ' is the effective friction angle, c' is the effective cohesion, α is the slope angle, γ is the material unit weight, γ_w is the unit weight of water, t is the slope-normal thickness of the failure slab, and m is the proportion of the slab thickness that is saturated. Substituting FS from Eq. (2) into Eq. (1) yields the critical acceleration k_c.

In order to calculate the cumulative permanent displacement triggered by ground shaking, a simple and accurate method proposed by Wilson and Keefer (1983) is used, where the permanent displacement is derived by double integrating those parts of the accelerations over the critical acceleration.

2.2 Seismic intensity

Peak ground acceleration (PGA) has been widely used as an earthquake shaking intensity measure. However, recently it has been recognized that the PGA is not an appropriate intensity measure in assessing structural damage. In order to accurately evaluate structural damage, several intensity measures have been proposed as follows.

Housner (1952) proposed a spectral intensity defined as:

$$\mathrm{SI}_{25}=\int_{0.1}^{2.5}\mathrm{PVRS}(T,\zeta)\mathrm{d}T \tag{3}$$

where SI_{25} represents the spectral intensity, PVRS(T, ζ) is the pseudo-velocity spectrum, PVRS(T,ζ)=($T/2/\pi$)*SA(T, ζ), here SA(T, ζ) is the spectral acceleration, T is the spectral period, and ζ is the damping ratio (here ζ=5%).

Arias (1970) proposed the following, called the Arias intensity, I_a

$$I_a=\frac{\pi}{2g}\int_0^{T_d}a^2(t)\mathrm{d}t \tag{4}$$

where $a(t)$ is the acceleration time history and T_d is the duration of the measured acceleration time history. The physical meaning of the Arias intensity is the input vibration energy.

Saragoni *et al*. (1989) also proposed a destructiveness potential (P_a) as an intensity measure, in which the effect of the vibration frequency, amplitude and duration of ground motions are considered

$$P_a=\frac{I_a}{2n^2} \tag{5}$$

where I_a is the Arias intensity and n is the number of zero crossings for the acceleration time history. The destructiveness potential has been used by Crespellani *et al*. (1998) in developing D_{LL} models.

3 New Zealand earthquake record data set

In the present study, the New Zealand strong motion data set that was used by Zhao *et al*. (1997) for the development of New Zealand PGA attenuation relationships and McVerry *et al*. (2006) for the development of New Zealand acceleration response spectra attenuation relationships is used, together with the implementation of some records from the 2003 Fiordland earthquake (a magnitude 7.2 event). In the original data set, some acceleroscope records and undigitized film records (only contributing to PGA

attenuation relationships) were included, but for the purpose of the D_{LL} attenuation model, those records were removed. Finally, 48 out of 52 events with earthquake moment magnitudes ranging from 5.0 to 7.2 remain

Table 1 New Zealand earthquakes considered in this study

No.	Date	UT	Epicentre		M_w	Centrum depth (km)	Tectonic type	Source mechanism	
			S	E					
1	1966-03-04	T23:58	38.45	177.91	5.64	24	I	R	
2	1966-04-23	T06:49	41.63	174.40	5.75	19	C	R	
3	1968-09-25	T07:02	46.49	166.68	6.27	4	C	S	
4	1971-08-13	T14:42	42.13	172.10	5.70	9	C	S	
5	1972-01-08	T21:33	37.57	175.69	7.27	7	C	N	
6	1973-01-05	T13:54	39.04	175.25	6.75	149	S	R	
7	1974-11-05	T10:38	39.65	173.63	5.44	17	C	N	
8	1975-06-10	T10:11	40.34	175.93	5.62	38	S	N	
9	1976-05-04	T13:56	44.67	167.45	6.51	10	C	R	
10	1977-01-18	T05:41	41.73	174.30	6.02	34	S	N	
11	1977-05-11	T02:41	43.26	171.73	5.20	10	C	S	
12	1979-03-24	T21:06	41.94	171.63	5.08	10	C	R	
13	1980-06-23	T16:45	39.90	175.60	5.49	61	S	R	
14	1980-10-05	T15:32	39.70	176.82	5.66	36	S	N	
15	1980-11-25	T04:57	37.78	178.97	5.54	41	S	N	
16	1982-02-05	T17:51	40.64	175.92	5.36	34	S	N	
17	1982-09-02	T15:58	39.74	176.93	6.46	31	S	N	
18	1984-03-05	T02:07	38.92	175.78	5.27	9	C	N	
19	1984-03-08	T00:40	38.31	177.29	5.91	80	S	R	
20	1984-06-24	T13:29	43.60	170.56	6.14	13	C	S	
21	1985-07-19	T14:33	38.72	177.30	5.92	31	S	N	
22	1987-03-02	T01:42	37.88	176.84	6.53	6	C	N	L
23	1988-06-03	T23:27	45.10	167.17	6.69	60	S	R	
24	1989-05-31	T05:54	45.27	166.88	6.33	24	I	S	
25	1989-08-08	T07:59	40.12	174.30	5.40	112	S	R	
26	1990-08-15	T15:54	40.32	176.44	5.17	28	S	N	
27	1990-10-04	T23:48	41.60	175.41	5.57	15	I	R	
28	1990-10-06	T02:41	41.60	175.41	5.46	15	I	R	
29	1991-01-28	T12:58	41.89	171.58	5.79	10	C	R	
30	1991-01-28	T18:00	41.90	171.67	5.93	11	C	R	
31	1991-02-15	T10:48	42.04	171.59	5.42	9	C	R	
32	1991-07-12	T04:42	39.31	175.97	5.30	69	S	S	
33	1991-09-08	T13:50	40.25	175.17	5.61	94	S	R	
34	1992-03-02	T09:05	40.31	176.48	5.54	26	S	N	
35	1992-03-30	T07:02	43.05	171.23	5.50	5	C	R	
36	1992-05-16	T17:57	38.23	178.37	5.76	22	I	R	
37	1992-05-27	T22:30	41.63	173.62	5.88	67	S	S	
38	1992-06-21	T17:43	37.67	176.83	6.25	4	C	N	
39	1993-04-11	T06:59	39.74	176.52	5.63	24	I	R	
40	1993-08-10	T00:51	45.21	166.71	6.81	22	I	R	L
41	1993-08-10	T09:46	38.52	177.87	6.19	39	S	S	L
42	1994-06-18	T03:25	43.01	171.46	6.81	4	C	R	L
43	1994-12-15	T11:20	37.27	177.53	6.31	12	C	S	
44	1995-02-05	T22:51	37.65	179.49	7.09	10	C	N	
45	1995-02-10	T01:45	37.92	179.51	6.49	10	C	N	
46	1995-03-22	T19:43	41.05	174.18	5.83	90	S	S	
47	1995-11-24	T06:19	42.98	171.80	6.24	5	C	S	
48	2003-08-21	T12:12	45.19	166.83	7.20	18	I	R	L

Note: Tectonic type: C = Crustal, I = Interface, S = Slab
Source mechanism: N = Normal, R = Reverse, S = Strike-slip
L = lots of Landslides triggered

and are listed in Table 1. Note that the modified data set covers different tectonic settings and earthquake fault types and includes several large earthquake events that triggered a broad range of landslides (Hancox *et al*., 1997, 2004) in New Zealand. The new data set is considered reasonable for developing D_{LL} attenuation models for mapping earthquake-induced landslide potential in New Zealand.

Significant factors for triggering of landslides have been studied. For example, Keefer (1984) pointed out that the minimum earthquake magnitude and the maximum epicentral distance for triggering landslides are, respectively, 5.2 and 500 km in terms of a global landslide data set; Hancox *et al*. (1997) also analyzed numerous landslides triggered by earthquakes in New Zealand and derived the minimum earthquake magnitude and the maximum epicentral distance as 5 and 175 km, respectively. In a recent study of landslides triggered by the 2003 Fiordland earthquake, Hancox *et al*. (2004) found that most of the landslides are concentrated within an epicentral distance of 60 km. On the basis of these past studies, the following two criteria are suggested in selecting accelerograms:

(1) The record should have a source distance of less than 175 km;

(2) The PGA of the record should be no less than 0.01g.

The first criterion is consistent with the study of Hancox *et al*. (1997, 2004). The second one refers to the models of Ambraseys and Srbulov (1994), where the minimum PGA is 0.1 g, but in the present study the minimum PGA is 0.01 g. The reasons for setting a lower bound of PGA are: 1) records with PGA greater than 0.1 g are limited in the New Zealand data set; and 2) setting a lower bound of PGA does not affect the final model, because slope stability is governed by the ratio of k_c/k_m; here k_m is the ground acceleration coefficient determined by PGA divided by gravity acceleration.

Similar to the discussions of the studies of Zhao *et al*. (1997) and McVerry *et al*. (2006), the data set has been supplemented with overseas near-source records to constrain the attenuation models at near-source distances where New Zealand recordings are sparse. In the study of McVerry *et al*., the overseas records from crustal earthquakes at source-to-site distances of 10 km or less were included. In this study, the overseas data set of McVerry *et al*. is used, and several records in the range 10 km to 20 km are added. The supplemented overseas records are listed in Table 2.

4 D_{LL} attenuation models using intensity measures

Intensity measures widely used in predicting D_{LL} are: 1) Arias intensity, I_a (Jibson *et al*. model (Jibson *et al*., 1998)); 2) PGA (Ambraseys and Srbulov model (Ambraseys and Srbulov, 1994)); and 3) destructiveness potential factor, P_a (Crespellani *et al*. model (Crespellani *et al*., 1998)). As mentioned above, the spectral intensity used in structural damage assessment is likely to be a valid intensity measure for predicting D_{LL} (explanations for this follow). At present, most D_{LL} attenuation models consist of different intensity measures, rather than a single one, such as Arias intensity and ratio of k_c/k_m or Arias intensity and k_c. Compared with term k_c, term k_c/k_m has a clearer physical meaning, namely that slope stability is dominated by the ratio. Consequently, the term k_c/k_m, rather than k_c, is used in this study. Therefore, the spectral intensity and k_c/k_m are both used to develop the D_{LL} attenuation model in this study by using the multi-linear regression method, as shown in Eq. (6). The attenuation model used herein was developed by using I_a and k_c/k_m as expressed in Eq. (7), with a similar functional form as the Romeo model (Romeo, 2000).

$$\log_{10} D_{LL}(\text{cm}) = 3.1199 + 0.8675\log_{10}(\text{SI}_{25})(\text{m}) - 3.50097(k_c/k_m) \quad (6)$$

Table 2 Other abroad earthquakes used in this study

No	Date	UT	Event name	M_w	Centrum depth (km)	Source mechanism
1	1940–05–19	T04:36	Imperial Valley	7.0	10	S
2	1966–06–28	T04:26	Parkfield	6.1	7	S
3	1971–02–28	T14:00	San Fernando	6.6	12	R
4	1978–08–13	T13:22	Santa Barbara	5.1	7	R
5	1978–09–16	T15:35	Tabas	7.41	11	R
6	1979–10–15	T23:16	Imperial Valley	6.5	10	S
7	1989–10–18	T00:04	Loma Prieta	6.92	12	S
8	1992–03–13	T17:18	Erzinch	6.72	10	S
9	1992–06–28	T11:57	Landers	7.36	7	S
10	1994–01–17	T12:30	Northridge	6.72	12	R
11	1995–01–16	T20:46	Hyogo-ken Nanbu	6.92	10	S

$$\log_{10}D_{LL}(\text{cm}) = 1.996 + 0.679\log_{10}(I_a)(\text{m/s}) - 3.298(k_c/k_m) \quad (7)$$

Standard deviations from Eqs. (6) and (7) are 0.3 and 0.37, respectively, in $\log_{10}$ scale. The difference between the two standard deviations is slight, but as mentioned above, the spectral intensity can be derived from PSHA and used to perform probabilistic seismic landslide analysis. This is why the spectral intensity is used to replace the Arias intensity in the D_{LL} attenuation model. Residuals of the predicted D_{LL} with respect to SI_{25} for the New Zealand earthquake record data set are shown in Fig.1, and an unbiased estimate is achieved.

To perform a sensitivity analysis, three existing D_{LL} attenuation models used in many studies are shown in Eq. (8). For comparison purposes, a relationship between the spectral intensity and Arias intensity is plotted in Fig. 2 and shown in Eq. (9), which is used to transform the Arias intensity to spectral intensity.

The Ambraseys and Srbulov model:

$$\log D_{LL}(\text{cm}) = 0.90 + 2.531\log(1 - k_c/k_m) - 1.09\log(k_c/k_m) \quad (8a)$$

The Jibson *et al.* model:

$$\log D_{LL}(\text{cm}) = 1.521\log I_a(\text{m/s}) - 1.9931\log k_c - 1.546 \quad (8b)$$

The Romeo model:

$$\log D_{LL}(\text{cm}) = 0.607\log I_a(\text{cm/s}) - 3.719(k_c/k_m) + 0.852 \quad (8c)$$

where k_c and k_m have the same meaning as in Eq. (6), and I_a is the Arias intensity.

$$\log(SI_{25})(\text{m}) = -1.2263 + 0.7631\log(I_a)(\text{m/s}) \quad (9)$$

Comparisons of the predicted D_{LL} are plotted in Figs. 3(a) and 3(b) with respect to Arias intensity and k_c/k_m, respectively. Figure 3(a) shows the effect of the input energy on the predicted D_{LL} for given slopes and PGAs, and Fig. 3(b) shows the effect of the critical acceleration coefficients of slopes on the predicted D_{LL} for a given acceleration time history. For a given k_c/k_m (see Fig. 3(a)), the new model predicts similar D_{LL} values to those of the Romeo model, but different from those of the Ambraseys and Srbulov and the Jibson

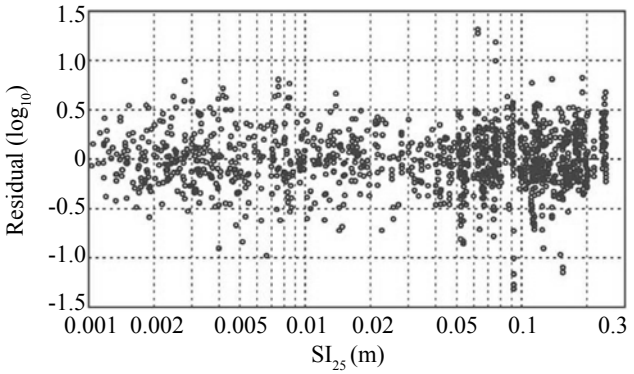

Fig. 1 Residuals of the predicted displacements in $\log_{10}$ scale based on Eq. (7) with respect to spectral intensity obtained from Eq. (3)

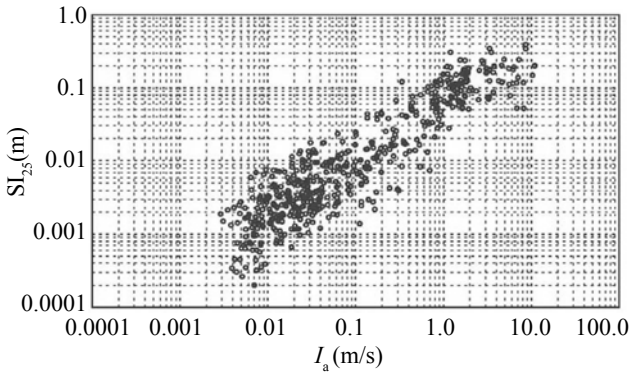

Fig. 2 Relationship between spectral intensity and Arias intensity derived from the New Zealand earthquake record dataset including crustal events and subduction zone events

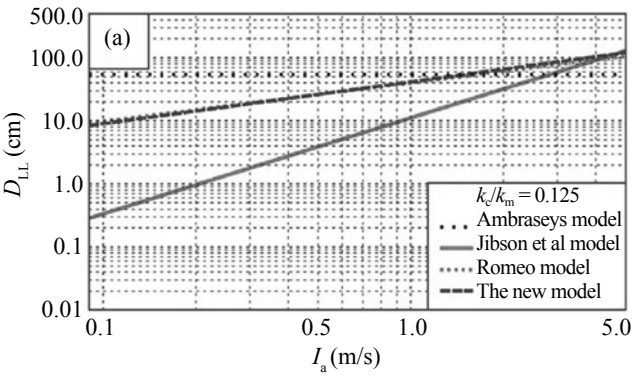

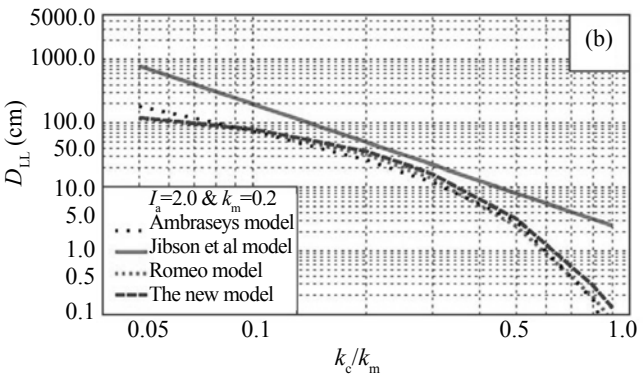

Fig. 3 Comparisons of displacements predicted from four different models in terms of Arias intensity and k_c/k_m

et al. models. The predicted D_{LL} from the Jibson *et al*. model is much lower than those from the other models for Arias intensities less than 3.0. The Ambraseys and Srbulov model includes only a parameter, k_c/k_m, and so the predicted D_{LL} is constant. For a given Arias intensity and k_m (see Fig. 3(b)), the predicted D_{LL} from the new model are similar to those from the Romeo model for most k_c/k_m values and slightly larger than those from the Ambraseys and Srbulov model for k_c/k_m larger than 0.1. The Jibson model provides upper bounds for the range of k_c/k_m considered. The similarity of the predicted D_{LL} between the new model and the Romeo model is likely to be because these two models have similar functional forms, and in addition, the Arias intensity and spectral intensity have a linear relationship on a logarithm scale, as shown in Eq. (9). For the Jibson model, the effect of k_m has been included in the Arias intensity, and so Fig. 3(b) for the Jibson model only shows a very special case. However, even for the special case, the predicted D_{LL} values of the Jibson model are close to those of the new model for a large range of k_c/k_m.

5 Development of D_{LL} attenuation models using earthquake source parameters

As discussed above, D_{LL} attenuation models were usually developed using various intensity measures (such as the Arias intensity), and these intensity measures have to be derived from corresponding attenuation relationships that are a function of source and path parameters (earthquake magnitude and source distance) and site conditions. In order to simplify the intermediate steps in predicting D_{LL}, the D_{LL} attenuation models are directly derived using earthquake source and path parameters by introducing three terms, one for site conditions, one for tectonic type and one for faulting mechanism, and are represented as:

$$\log_{10}(D_{LL})(\text{cm}) = 5.7949M_w - 0.4084{M_w}^2 - 0.4244\log_{10}\left({r_{rup}}^2 + 0.02\times 10^{0.45M_w}\right) - 3.4323(k_c/k_m) + 0.1215\times \text{SC} - 17.5128 \quad (10)$$

where M_w is the moment magnitude, r_{rup} is the shortest distance to the rupture plane from the recording station in km, and SC is a dummy variable for site condition, 0 for rock sites and 1 for soil sites. Note that in Eq. (10) only the site condition effect is explicitly included (in order to compare with existing models). Furthermore, the maximum magnitude used in developing the model is 7.4, therefore the upper limitation of magnitude for using the model is 7.0. The first three terms on the right side of the equation include the effect of earthquake magnitude and source distance. In log(distance) term, a magnitude-dependent term is added for reflecting the phenomena of magnitude saturation at near-fault sites. In addition, a magnitude-square term is introduced in the model to reduce the bias of residuals with respect to magnitude.

The standard deviation, $\sigma_{\log_{10}D_{LL}}$, of the model is 0.39. In this study, rock sites contain subsoil category (a) in New Zealand Standard NZS4203:1992 (1992) with natural periods less than 0.25 s, and soil sites contain subsoil categories (b) and (c). Residuals of predicted D_{LL} with respect to earthquake magnitude and distance are shown in Fig. 4. Figure 4 shows that an unbiased estimate for earthquake magnitude has been achieved.

For comparison purposes, the Ambraseys and Srbulov model (1994) and Romeo model (2000) are listed below:

Ambraseys and Srbulov model:

$$\log D_{LL}(\text{cm}) = 0.463M_s - 0.008\sqrt{r^2+h^2} + \log\left[\left(1-k_c/k_m\right)^{2.58}(k_c/k_m)^{-1.07}\right] - 2.4 \quad (11a)$$

Romeo model:

$$\log D_{LL}(\text{cm}) = 0.591M - 0.852\log\left(\sqrt{{r_{rup}}^2 + 2.6^2}\right) - 3.703(k_c/k_m) + 0.246\text{SC} - 1.144 \quad (11b)$$

where M_s is the surface-wave magnitude, r is the horizontal site-source distance in km, h is the focal depth in km, r_{rup} is the shortest distance to rupture plane,

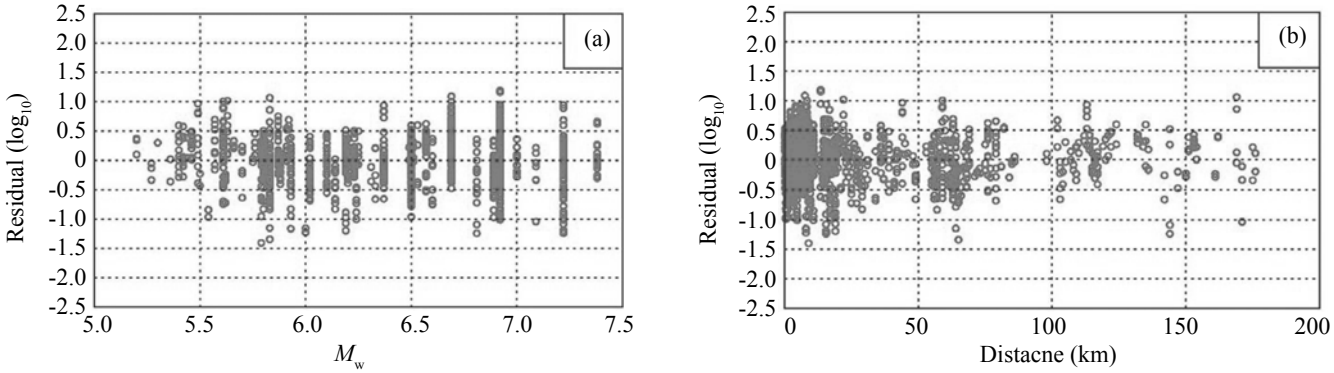

Fig. 4 Residuals with respect to (a) earthquake magnitude and (b) source distance from predictive displacement model Eq. (10). (maximum source distance = 175 km)

and SC in the Romeo model is a dummy factor, 1 for soil sites and 0 for rock sites, M in the Romeo model refers to local magnitude for $M \leq 5.5$ and surface wave magnitude for $M > 5.5$. Other parameters have the same meaning as in Eq. (10). Note that the Ambraseys and Srbulov model does not account for the effect of site conditions. Figure 5 shows a comparison of the predicted D_{LL} by the three models for magnitude 5.8 and 6.8 events on soil sites, the latter of which is the maximum event in the Romeo data set.

For the magnitude 5.8 event, the predicted D_{LL} values from the new model (Eq. (10)) and Romeo model are similar for most source distances, but a slightly difference occurs at short source distances. At source distances between 10–100 km, the predicted D_{LL} values by the Ambraseys and Srbulov model are close to those of the new model, but at source distances less than 10 km, the Ambraseys and Srbulov model predicts much lower D_{LL} values than those from the new model. For the magnitude 6.8 event, the Romeo model predicts larger D_{LL} values than those of the new model at source distances less than 5 km, and for distances larger than 5 km, the two models predict similar D_{LL} values. However, the predicted D_{LL} values from the Ambraseys and Srbulov model are much lower than those from the new model and the Romeo model for source distances less than 15 km. It is worth noting that the difference in the predicted D_{LL} of the three models exists mainly at short source distances. Generally speaking, near-fault prediction is mainly dominated by the near-fault records used in developing the model. Therefore, the difference is likely that different near-fault records were used in the three models. On the other hand, the Ambraseys and Srbulov model uses the horizontal site-source distance, but the other two models use the shortest distance to rupture plane. Therefore, some differences between the Ambraseys and Srbulov model and the new model are also attributed to different source distances used. Note also that for the three models, different magnitudes have been used, but for the 5.8 and 6.8 magnitude events, the error caused by using different magnitudes can be ignored with respect to the other two as mentioned above.

Strong motion attenuation models have shown that crustal and subduction zone earthquakes produce different ground motions (Zhao *et al*., 2006). For example, subduction zone earthquakes generally produce stronger high frequency responses than crustal earthquakes. Therefore, the New Zealand earthquake record data set was divided into two groups based on crustal earthquake events and subduction zone earthquake events, respectively. The subduction zone earthquake events were not further divided into interface and intra-slab events because of the lack of data, although these two types of earthquakes produce different ground surface shaking. For crustal earthquake events, the data is again divided into two subgroups based on faulting mechanism, one for strike-slip and normal faulting

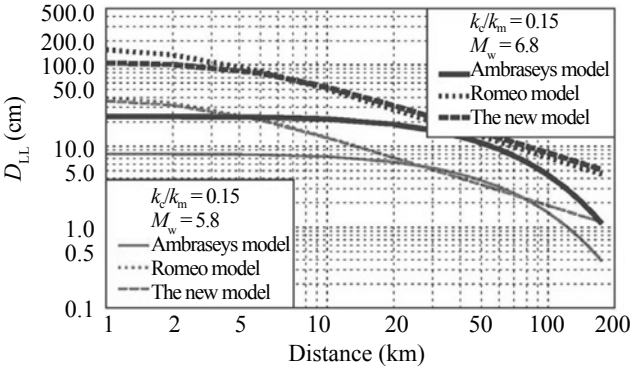

Fig. 5 Comparisons of displacements predicted from three different models in terms of earthquake source parameters for earthquake magnitudes of 5.8 and 6.8 on a soil site

and the other for reverse faulting. The effect of site conditions is also taken into account. The D_{LL} models for crustal events and subduction zone events are shown in Eqs. (12) and (13). Note that Eqs. (12) and (13) are only used for moment magnitudes less than 7.0, and Eq. (11b) can be used directly for a moment magnitudes larger than 7.0, because for a moment magnitude less than 7.0, Eq. (12) and Eq. (11b) obtain similar values.

For crustal events:

$$\log(D_{LL})(\text{cm}) = 6.7122M_w - 0.4756M_w^2 - 0.4497\log\left(r_{rup}{}^2 + 0.02\times10^{0.45M_w}\right) - 3.5446(k_c/k_m) + 0.04571\,\text{SR} + 0.1305\,\text{SC} - 20.5559 \quad (12)$$

where SR is the fault type term, 0 for strike slip or normal faulting and 1 for reverse faulting, and M_w, r_{rup}, SC is defined in Eq. (10). This model has a standard deviation, $\sigma_{\log_{10}D_{LL}}$, of 0.38. From Eq. (12), it is known that reverse faulting produces a D_{LL} about 11% larger than that from strike slip or normal faulting for the same site condition, and the displacement on soil sites is about 35% larger than on rock sites for the same earthquakes .

For subduction zone events:

$$\log(D_{LL})(\text{cm}) = 3.5722M_w - 0.24M_w^2 - 0.2744\log\left(r_{rup}{}^2 + 0.02\times10^{0.45M_w}\right) - 2.8879(k_c/k_m) + 0.2071\,SC - 11.0208 \quad (13)$$

where M_w, r_{rup}, SC is defined in Eq. (10). The standard deviation of Eq. (13) is 0.39. It is clear that the scatter for directly predicting D_{LL} using earthquake source and path parameters is larger than that using SI_{25} which has a standard deviation of 0.3. Equation (13) shows that the displacement D_{LL} on soil sites is about 61% larger than that on rock sites for the same earthquakes. The difference in D_{LL} values for two site conditions is mainly attributed to the contribution of high frequencies

to D_{LL}, which is small on rock sites, while the soil site amplification to seismic waves dominates the D_{LL} values on soil sites.

6 Validation of the new D_{LL} attenuation models

To verify the developed D_{LL} attenuation models, a commonly used approach is to compare predicted and observed D_{LL} values. Al-Homoud and Tahtamoni (2000) investigated two landslides triggered by earthquakes. One is the Lower San Fernando dam landslide triggered by the 1994 magnitude 6.7 Northridge earthquake (Bardet and Davis, 1996) at a short source distance of about 6.5 km. The other is the Andretta landslide triggered by the 1980 magnitude 6.5 Irpinia earthquake (D'ella, 1992) at a short source distance of about 0.5 km. The critical accelerograms for the Lower San Fernando dam landslide were determined by Bardet and Davis (1996), and the critical accelerograms for the Andretta landslide were determined by Al-Homoud and Tahtamoni.

Figure 6 shows a comparison between the predicted displacements from the new D_{LL} model (Eq. (12)), the Ambraseys and Srbolov model (Eq. (11a)), the Romeo model (Eq. (11b)), and the measured displacements from the Lower San Fernando dam landslide and the Andretta landslide.

Note that all the models underestimate the landslide displacements. A probable reason may be that in these models, near-fault effects and amplification by the hills were not taken into account. However, Fig. 6 gives us confidence that the trend of the predicted D_{LL} values with respect to k_c/k_m is quite similar to that of the measured displacements, i.e., the displacement reduces with increasing k_c/k_m. In Fig. 6, curves representing mean values plus and minus one standard deviation from the new model are also provided. It shows that these curves fit the data very well. Considering the possible near-fault effects that may enhance the measured displacement, the new model can be reliable for sites without near-fault effects. The comparison also shows that the predicted D_{LL} values from the new model Eq. (12) are close to those from the Romeo model.

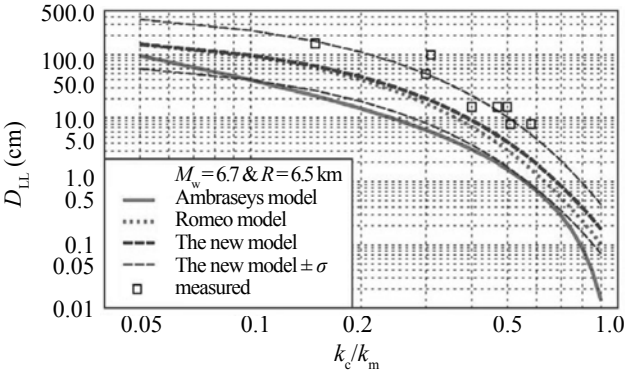

Fig. 6 Comparisons of measured displacements and displacements predicted from three different models for the 1994 Northridge earthquake of M = 6.7

Romeo (2000) also reported some measured landslide displacements triggered by the 1980 magnitude 6.9 Irpinia earthquake. Some parameters used by Romeo are listed in Table 3, where the D_{LL} values predicted by the new model are also provided. The comparison shows that the new model predicted D_{LL} values close to those from the observed and calculated displacements. The latter was derived from site-specific studies.

In the 2008 Wenchuan earthquake, many landslides were triggered. Measurements were obtained from two landslides, including landslide volume, size and slope angle. One landside is located near the ABa aluminium manufacturing facility and the other is located near the Youyi Tunnel (1 km in the Yingxiu direction). The landslide near the ABa aluminium manufacturing facility was 50 m long, had a bottom width of 50 m, a thickness of 4 m, a rock-base slope of 50°, and a sliding displacement of 5 m. The landslide near the Youyi Tunnel was 500 m long, had a bottom width of 120 m, an upper width of about 75 m, rock-base slope of 50°, and a sliding displacement of 4 m. In the analysis, peak ground acceleration (PGA) for the two landslides is taken as 0.975 g, which was recorded at the Wolong station. The PGA was taken from Wolong station because both landslides have a distance to fault plane similar to the

Table 3 Comparisons of the observed (or calculated) D_{LL} values: triggered by the 1980 Irpinia earthquake and predicted by the Romeo model (Eq. (11b)) and the new model (Eq. (12))

Locality of landslide	Closest distance (km)	k_c/k_m	Observed or calculated* displacements (cm)	Reome model Eq. (11b)	New model Eq. (12)
Calitri	20	0.07	55*	56	63
Andretta	17	0.07–0.15	70–20*	65–33	72–38
Buonin-ventre	3	0.08	General collapse	174	185
Senerchia	9	0.06	General collapse	118	129
Pergola	9	0.16	≈30	50	57
S.Giorgio La Molara	40	0.24	Ground cracks	7	8

*Note** : From site-specific analysis

Wolong station. From the measured soil strength and Eq. (2), a critical acceleration of 0.13 g is calculated. Finally, the calculated displacements are 4.53 m for the landslide near the ABa aluminium facility and 3.35 m for the landslide near the Youyi Tunnel. The comparison shows that the calculation slightly underestimates the landslide displacement, which may be because the near-fault effect is neglected and few larger earthquake events are included in the model.

7 Probabilistic seismic D_{LL} analysis by using the new model

Probabilistic seismic landslide displacement analysis (PSLDA) has been given attention in recent years, but because of its complexity, little progress in PSLDA has been made. However, to apply PSLDA to map landslide potential, an approximate method has been proposed by Romeo (2000), in which the intensity measures, corresponding to different earthquake return periods, are estimated from probabilistic seismic hazard analysis (PSHA), and then the estimated intensity measure is substituted into D_{LL} attenuation models (such as Eq. (6)). Romeo (2000) applied the method to map landslide displacements, and attained the Arias intensity with 10% probability of exceedance in 50 years. However, at present, PSHA often outputs 5% damped elastic acceleration spectra, thus directly deriving the spectral intensity is more convenient, compared to deriving other intensity measures by considering hazard probability. Therefore, in the D_{LL} attenuation models, using the spectral intensity as a parameter is an alternative for performing PSLDA, except for using Arias intensity. The steps for using Eq. (6) to derive PSLDA are as follows:

Step 1: calculate 5% damped elastic pseudo-velocity spectrum PVRS(T) based on the 5% damped elastic acceleration spectrum SA(T) from PSHA;

Step 2: calculate spectral intensity by integrating the pseudo-velocity spectra in a period range of 0.1 s to 2.5 s; and

Step 3: estimate D_{LL} using Eq. (6), in which the k_m can be directly obtained from the estimated acceleration spectra.

The procedure above is similar to that of Romeo (2000), except that the spectral intensity is used to derive PSLDA. Note that the standard deviation used in PSHA is that of spectral acceleration attenuation models, and the standard deviations of most spectral acceleration attenuation models are close to that of the new model (Eq. (6)) (For example, the McVerry *et al*. model (2006) has σ_{log10}= 0.26 and the Japan attenuation model (Zhao *et al*., 2006) has σ_{log10}= 0.34). Therefore, the methodology that using the standard deviation in the spectral acceleration attenuation model derives acceleration spectra, and then the estimated acceleration spectra are used to estimate D_{LL} values is believed to be appropriate.

To show the difference between deterministic landslide displacement analysis and PSLDA, an example is provided. In the example, spectral intensities are calculated from the New Zealand probabilistic seismic hazard model (Stirling *et al*., 2002) and D_{LL} is estimated from the D_{LL} attenuation model (Eq.(6)).

The site is located in Wellington, one of the high seismic hazard regions in New Zealand. Three faults make major contributions to the Wellington seismic hazard. The Wellington fault has the potential to produce a magnitude 7.3 earthquake with a recurrence interval of about 600 years, the Wairarapa fault produced a magnitude 8.1 earthquake event in 1855 with a recurrence interval about 1,500 years, and the Ohariu fault produced a magnitude 7.4 earthquake event in history with a recurrence interval about 3,250 years. Other sources also contributed to the seismic hazard of the site, such as the North Island subduction zone and distributed seismicity. The site conditions are classified as subsoil category (b) (intermediate soil sites) based on NZS1992:4203 (1992). Figure 7 shows 5% damped elastic acceleration spectra with 150-, 475- and 1,000-year return periods and the 50-percentile spectrum produced by the Wellington

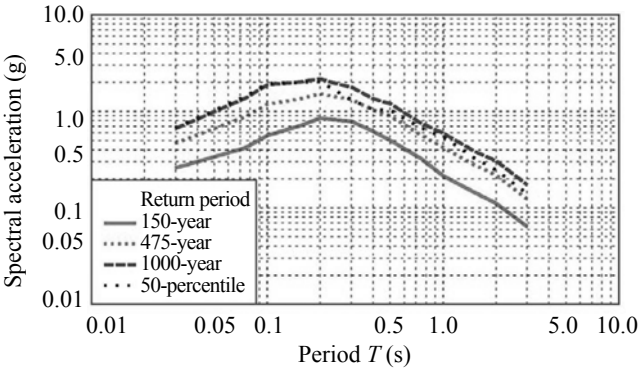

Fig. 7 Estimated 5% damped elastic acceleration spectra derived from New Zealand probabilistic seismic hazard model for return periods of 150, 475 and 1000 years and 50-percentile ground motion at Lower Hutt

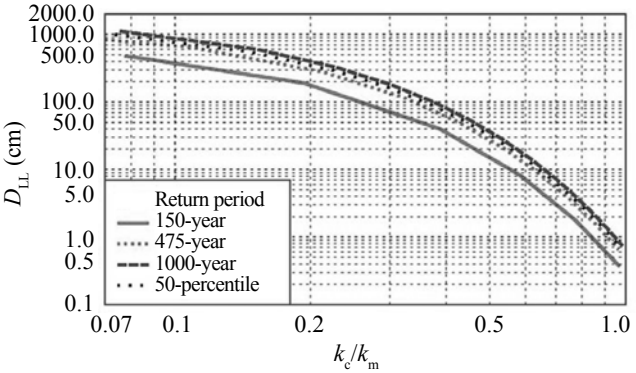

Fig. 8 Displacements for different earthquake return period predicted from combining the new model and New Zealand probabilistic seismic hazard model with respect to k_c/k_m

fault. Figure 8 shows the variation of the predicted D_{LL} with respect to k_c/k_m for these return periods and the 50-percentile ground motion. In the calculations, a suite of critical accelerations have been given, with an assumption that these critical accelerations correspond to a suite of slopes.

Note that for PSLDA, the estimated D_{LL} values are dependent on earthquake return period. As expected, the longer the return period, the larger the seismic hazard level, and so the larger the landslide displacement. The D_{LL} values from the 50-percentile ground motion are between those from the 475- and 1000-year return periods. The results show that the predicted D_{LL} by the deterministic analysis and PSLDA are different. Therefore, the PSLDA method, which includes various uncertainties, should be developed.

8 Conclusions

This study focuses on developing two types of landslide displacement attenuation models. One uses intensity measurements and is applicable to probabilistic seismic landslide displacement analysis. The other uses earthquake parameters and accounts for the effect of tectonic settings and faulting mechanism. A detailed comparison between the Ambraseys and Srbulov model (Eq. (11a)), the Romeo model (Eq. (11b)) and the developed model (Eq. (10)) was made. The following conclusions are achieved from this study:

(1) A landslide displacement attenuation model using spectral intensity as a parameter is developed, and the merits of using the spectral intensity are: 1) the spectral intensity contains the effects of spectral amplitude and spectral frequency; and 2) the probabilistic seismic landslide displacement analysis can be easily carried out, as the spectral intensity is obtained based on the acceleration spectra derived from probabilistic seismic hazard models.

(2) The landslide displacements predicted from the new model are close to those from the Romeo model, and larger than those from the Ambraseys and Srbulov model. The difference in the predicted D_{LL} values between the new model and the Ambraseys and Srbulov model may originate from using different functional forms and earthquake record data sets.

(3) The new models expressed by earthquake source parameters (Eqs. (12) and (13)) account for the effect of crustal and subduction zone earthquakes by introducing a tectonic type term. For crustal earthquakes, strike-slip or normal faulting and reverse faulting are accounted for based on a fault term. For all models, site conditions have been accounted for based on soil and rock site conditions. Generally, the displacement triggered by reverse faulting is about 18% larger than that of strike-slip faulting on soil sites and about 32% larger on rock sites.

(4) An example is provided which shows how to use the landslide displacement attenuation model (Eq. (6)) to perform probabilistic seismic landslide analysis. The example shows that the predicted displacements differ for different earthquake return periods, and the displacements derived from the 50-percentile ground motion is between those from 475- and 1,000-year return periods. Based on this simple methodology, mapping probabilistic seismic landslide potential becomes convenient.

(5) Comparisons between predicted and measured landslide displacements triggered by earthquakes suggest that the new models, including those expressed by either spectral intensity or earthquake source parameters, provide acceptable displacement estimates, particularly for displacements with respect to the ratio of critical acceleration coefficient to ground acceleration coefficient.

Acknowledgement

The authors wish to thank Dr. Zhao JX, Hancox GT, Dellow G, and D. Beetham for discussions in this study and reviewing the manuscript. This study was supported in part by the Foundation for Research and Science and Technology of New Zealand, Contract number C05X0208 and C05X0301 and the Major Project of Chinese National Programs for Fundamental Research and Development (973 Program), Contract number 2008CB425802.

References

Al-Homoud AS and Tahtamoni W (2000), "Comparison Between Predictions Using Different Simplified Newmarks' Block-on-plane Models and Field Values of Earthquake Induced Displacements," *Soil Dyn. Earthquake Engng.*, **19**: 73–90.

Ambraseys NN and Srbulov M (1994), "Attenuation of Earthquake-induced Ground Displacements," *Earthquake Engineering and Structural Dynamics*, **23**: 467–487.

Arias AA (1970), "Measure of Earthquake Intensity," Hansen RJ, *Seismic Design for Nuclear Power Plants*, Massachusetts Institute of Technology.

Bardet JP and Davis CA (1996), "Performance of San Fernando Dams during 1994 Northridge Earthquake," *J Geotech Engng.*, **122**(7): 554–564.

Crespellani T, Madiai C and Vannucchi G (1998), "Earthquake Destructiveness Potential Factor and Slope Stability," *Geotechnique*, **48**(3), 411–419.

D'ella B (1992), "Dynamic Aspects of Landslide Reactivated by the 23 November 1980 Irpinia Earthquake (South Italy)," *Proceedings of the French-Italian conference of Slope Stability in Seismic Areas*.

Hancox GT, Cox SC, Turnbull IM and Crozier MJ (2004), "Landslides and Other Gground Damage Caused

by the M_w 7.2 Fiordland Earthquake of 22 August 2003," Farguhar G, Kelsey P, Marsh J, Fellows D, *Proceedings of the 9th Australia and New Zealand Conference on Geomechanics*, University of Auckland, New Zealand, 747–753.

Hancox GT, Perrin ND and Dellow GD (1997), "Earthquake-induced Landslides in New Zealand and Implications for MM Intensity and Seismic Hazard Assessment, *Client Report 43601B* Institute of Geological & Nuclear Sciences, December 1997, Prepared for Earthquake Commission Research Foundation.

Housner GW (1952), "Spectral Intensities of Strong Motion Earthquakes," *Proceedings of the Symposium on Earthquakes and Blast Effects on Structures*, Earthquake Engineering Research Institute.

Jibson RW, Harp EL and Michael JA (1998), "A Method for Producing Digital Probabilistic Seismic Landslide Hazard Maps: An Example from the Los Angeles, California Area," *Report 98-113*, US Geological Survey O-F.

Keefer DK (1984), "Landslides Caused by Earthquakes," *Geological Society of America Bulletin*, **95**: 406–421.

McVerry GH, Zhao JX, Abrahamson NA and Somerville PG (2006), "New Zealand Acceleration Response Spectrum Attenuation Relations for Crustal and Subduction Zone Earthquakes," *Bulletin of the New Zealand Society for Earthquake Engineering*, **39**(1): 1–58.

New Zealand Standards (1992), *NZS4203:1992 Loadings Standard, Code of Practice for General Structural Design and Design Loadings for Buildings*.

Newmark NM (1965), "Effects of Earthquakes on Dams and Embankments," *Geotechnique*, **15**(2), 139–160.

Romeo R (2000), "Seismically Induced Landslide Displacements: a Predictive Model," *Engineering Geology*, **58**(12): 337–52.

Saragoni R, Holmberg, A and Saez A (1989), "Potential Destructivy Destructividad del Terremoto del Chile de 1985," *Proceedings of Sas Jorn Chilenas de Sismologiae Ing Antisismica*, **1**: 369–378.

Stirling MW, McVerry GH and Berryman KR (2002), "A New Seismic Hazard Model for New Zealand," *Bulletin of the Seismological Society of America*, **92**(5): 1878–1903.

Wartman J, Seed RB and Bray JD (2001), "Physical Model Studies of Seismical Induced Deformations in Slopes," *GeoEngineering Report No. UCB/GT/01-01, January 2001*, Geo-Engineering, Department of Civil and Environmental Engineering, University of California, Berkeley.

Wilson RC and Keefer DK (1983), "Dynamic Analysis of Slope Failure from the 6 August 1979 Coyote Lake, California Earthquake," *Bulletin of the Seismological Society of America*, **73**: 863–877.

Zhao JX, Dowrick DJ and McVerry GH (1997), "Attenuation of Peak Ground Accelerations in New Zealand Earthquakes," *Bulletin of the New Zealand National Society for Earthquake Engineering*, **30**(2): 133–158.

Zhao JX, Zhang J, Asano A, Ohno Y, Oouchi T, Takahashi T, Ogawa H, Irikura K, Thio HK, Somerville PG, Fukushima Y and Fukushima Y (2006), "Attenuation Relations of Strong Ground Motion in Japan Using Site Classification Based on Predominant Period," *Bulletin of Seism. Soc. of America*, **96**(2): 898–913.